- Technical Paper -

A STUDY ON THE FAILURE PROPERTIES OF CEMENTITIOUS COMPOSITES REINFORCED WITH ORGANIC AND STEEL FIBER UNDER COMPLEX LOADS

Yaechan LEE*1, Gyuyong KIM*2, Hamin EU*1 and Jeongsoo NAM*2

ABSTRACT

This study examines hybrid fiber-reinforced cementitious composites (HP-HFRCC) with polypropylene (PP) and smooth steel fibers (SSF) under high-temperature and high-velocity impact conditions. Specimens tested from 25°C to 700°C showed hybrid-reinforced types (Fc100PPSF, Fc140PPSF) excelled in spalling, scabbing, and penetration resistance. Adding 0.15% PP and 1% SSF reduced mass loss and fractures, proving HP-HFRCC's value for disaster-resilient smart city infrastructure with enhanced durability.

Keywords: cementitious composites, fiber reinforced, thermal exposure, impact loading

1. INTRODUCTION

Smart cities represent a new paradigm of urbanization aimed at achieving carbon neutrality, industrial efficiency, and enhanced convenience in modern life. These cities are implemented through eco-friendly elements such as sustainable energy charging systems, carbon-reducing transportation, and zero-energy buildings. Characterized by hyper-connectivity enabled by massive IoT networks and advanced communication systems, smart cities strive to maximize urban convenience while minimizing environmental impact. However, the technologically intensive environment and high population density make smart city infrastructures highly vulnerable in disaster scenarios, particularly when high-energy loads, such as fires, occur, potentially causing large-scale damage[1-2].

Electric vehicles (EVs), a hallmark of smart city transportation, exemplify this risk. EVs powered by lithium-ion batteries (LIBs) inherently possess high energy densities, posing significant hazards during fires, including the potential for secondary explosions. Furthermore, the nature of smart cities often places EV charging stations and parking facilities underground, where confined spaces exacerbate fire risks and introduce dynamic loads that accelerate the deterioration and failure of concrete structures. Similar compounded stresses are evident in extreme scenarios such as nuclear plant accidents, hydrogen station explosions, and attacks involving terrorism or warfare. For instance, the 2020 Beirut port explosion demonstrated the catastrophic structural damage caused by high temperatures and impact loads[3-5].

The majority of smart city structures are composed of high-strength concrete (HSC) and ultra-high-performance concrete (UHPC), materials that provide superior strength and durability[6-7]ever, these materials are prone to spalling under high-temperature conditions due to increased internal vapor pressure. To mitigate this issue, cementitious composites reinforced with thermoplastic fibers (PE, PVA, PP) have been developed. Among these, polypropylene fibers (PP) are particularly noteworthy for their cost-effectiveness and substantial improvement of fire resistance with minimal content. Nevertheless, PP alone are insufficient to significantly enhance the tensile properties of concrete. Combining PP with steel fibers has been identified as a critical approach, as steel fibers improve stress distribution and crack control, enhancing resistance to dynamic loads. However, the presence of steel fibers can increase the risk of spalling at high temperatures.

To address these challenges, hybrid fiber-reinforced high-performance cementitious composites (HP-HFRCCs), incorporating both PP and steel fibers, have been proposed. These composites offer superior resistance to high temperatures and dynamic loads. Studies indicate that an optimal combination of 1% steel fibers and 0.15–0.2% PP fibers by volume can achieve high strength capacity while maintaining low pore pressure. Despite these advancements, most research has focused on single-load conditions, leaving a knowledge gap regarding the performance of these materials under combined high-temperature and dynamic load scenarios. This gap is particularly critical for understanding the localized impact of collisions during fire or explosion events, which can occur in disaster situations[8].

This study aims to experimentally analyze the failure characteristics of HP-HFRCC reinforced with polypropylene fibers (PP) and smooth steel fibers (SSF) under thermal degradation and high-velocity impact loads. Specimens were tested under various temperatures and impact conditions to evaluate residual mechanical properties and failure behaviors. The study further examines whether HP-HFRCC can demonstrate superior protective performance under reduced thickness compared to conventional materials. These findings are expected to contribute to enhancing the resilience of smart city infrastructures and provide foundational data for designing effective protective systems under disaster conditions.

*1 Ph.D Course, Dept. of Architecture Engineering, Chungnam National University, Rep. of Korea, JCI Member
*2 Prof., Dept. of Architecture Engineering, Chungnam National University, Rep. of Korea, JCI Member

Table 1 Mechanical properties of the used fibers

Type	Mechanical properties
Polypropylen fiber (PP)	Length: 12 mm, Daimeter: 42.6 μm, Aspect ratio(L/D): 281.7, Density: 0.91 g/cm^2, Tesnsile strength: 560 MPa
Smooth steel fiber (SSF)	Length: 16.3 mm, Daimeter: 200 μm, Aspect ratio(L/D): 81.5, Density: 7.85 g/cm^2, Tesnsile strength: 2700 MPa

Table 2 Mix proportion

ID.	F_{ck} (MPa)	Fiber content PP	Fiber content SSF	Mix proportions (kg/m^3) W/B	C	W	SS[1]	GGBS[2]	SF[3]	SP[4]
Fc 100N	100	0.00	0.00	0.25	770	250	845	155	75	230
Fc 100PP		0.15	0.00							
Fc 100PPSF		0.15	1.00							
Fc 140N	140	0.00	0.00	0.20	800	200	880	0	200	240
Fc 140PP		0.15	0.00							
Fc 140PPSF		0.15	1.00							

[1] Silica sand, [2] Ground Granulated Blast-furnace Slag, [3] Silica fume, [4] Silica powder

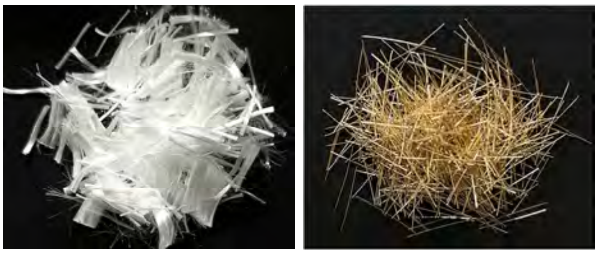

(a) Polypropylene (PP) (b) Smooth steel fiber (SSF)

Fig.1 Used fibers

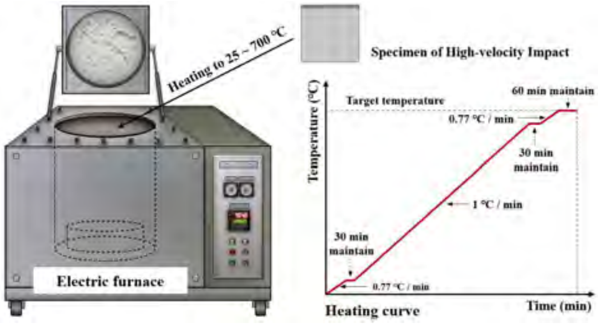

Fig.2 Electric furnace and heating temperature set up

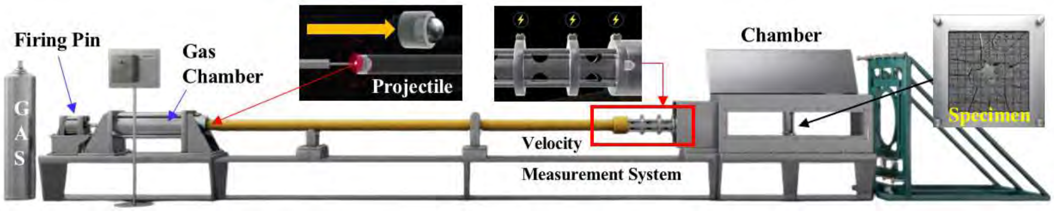

Fig.3 High-velocity projectile impact test machine

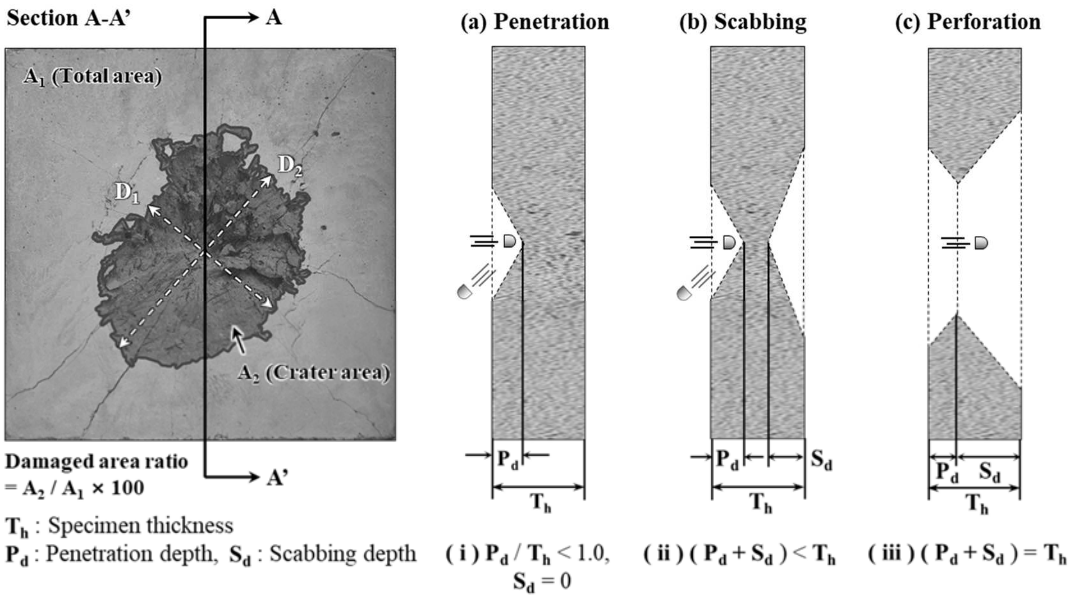

Fig.4 Method for evaluating crater diameter and fracture depth

2. TEST PROGRAMS

This study focuses on evaluating the protective performance of hybrid fiber-reinforced high-performance cementitious composites (HP-HFRCC) under thermal degradation and high-velocity impact conditions. The experiments were designed to assess the residual impact resistance of specimens reinforced with polypropylene fibers (PP) and smooth steel fibers (SSF). Thermal loads were applied using an electric furnace at five target temperatures up to 700°C. Specimens were maintained at each target temperature for a specific duration to simulate thermal degradation. Subsequently, high-speed projectile impact tests were conducted on the thermally degraded specimens to evaluate their impact resistance under extreme conditions.

The physical properties of the fibers used in HP-

Table 3 Failure levels of the 40 mm thickness specimens after heating and impact tests.

Specimen ID.	Fc100N	Fc140N	Fc100PP	Fc140PP	Fc100PPSF	Fc140PPSF
Temperature	Front / Rear	Front / Rear	Front / Rear	Front / Rear	Front / Rear	Front / Rear
25℃	Perforation (L6)	Perforation (L6)	Perforation (L6)	Perforation (L6)	Scabbing (L4)	Penetration (L3)
100℃	Perforation (L6)	Perforation (L6)	Perforation (L6)	Perforation (L6)	Scabbing (L4)	Penetration (L2)
200℃	Perforation (L6)	Perforation (L6)	Perforation (L6)	Perforation (L6)	Scabbing (L4)	Penetration (L2)
300℃	Perforation (L6)	Perforation (L6)	Perforation (L6)	Perforation (L6)	Scabbing (L4)	Penetration (L2)
500℃	Explosive spalling	Explosive spalling	Perforation (L6)	Perforation (L6)	Perforation (L5)	Penetration (L3)
700℃	Explosive spalling	Explosive spalling	Perforation (L6)	Perforation (L6)	Perforation (L6)	Perforation (L5)

Table 4 Failure levels of the 60 mm thickness specimens after heating and impact tests.

Specimen ID.	Fc100N	Fc140N	Fc100PP	Fc140PP	Fc100PPSF	Fc140PPSF
Temperature	Front / Rear	Front / Rear	Front / Rear	Front / Rear	Front / Rear	Front / Rear
25℃	Perforation (L6)	Perforation (L6)	Perforation (L6)	Perforation (L6)	Penetration (L3)	Penetration (L2)
100℃	Perforation (L6)	Perforation (L6)	Scabbing (L4)	Perforation (L6)	Penetration (L2)	Penetration (L2)
200℃	Perforation (L6)	Perforation (L6)	Scabbing (L4)	Perforation (L6)	Penetration (L2)	Penetration (L2)
300℃	Perforation (L6)	Perforation (L6)	Scabbing (L4)	Perforation (L6)	Penetration (L3)	Penetration (L2)
500℃	Explosive spalling	Explosive spalling	Perforation (L6)	Perforation (L6)	Penetration (L3)	Penetration (L2)
700℃	Explosive spalling	Explosive spalling	Perforation (L6)	Perforation (L6)	Scabbing (L4)	Penetration (L3)

HFRCC are summarized in Table 1 and Fig. 1. The reinforcing fibers consist of PP and SSF. PP have a length of 12 mm, a diameter of 42.6 μm, and an aspect ratio of 281.7, while SSF have a length of 16.3 mm, a diameter of 200 μm, and an aspect ratio of 81.5. PP despite their low density and strength, were adopted for their effectiveness in preventing spalling at high temperatures. SSF fibers, with their superior mechanical properties, are expected to enhance impact resistance. The presence of silica fume and silica powder facilitates pozzolanic reactions, and the reaction products improve cement properties while efficiently filling capillary spaces, thereby increasing the

Table 5 Failure levels of the 80 mm thickness specimens after heating and impact tests.

Specimen ID.	Fc100N		Fc140N		Fc100PP		Fc140PP		Fc140PPSF		Fc140PPSF	
Temperature	Front	Rear	Front	Rear	Front	Rear	Front	Rear	Front	Rear	Front	Rear
25°C												
	Perforation (L5)		Perforation (L6)		Scabbing (L4)		Scabbing (L4)		Penetration (L1)		Penetration (L1)	
100°C	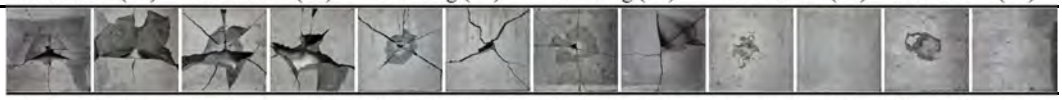											
	Perforation (L5)		Perforation (L6)		Scabbing (L4)		Scabbing (L4)		Penetration (L1)		Penetration (L1)	
200°C	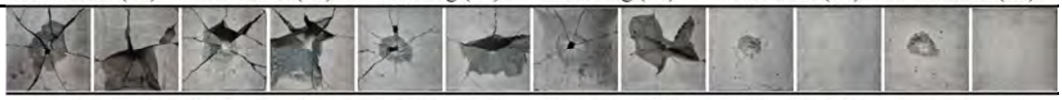											
	Scabbing (L4)		Perforation (L6)		Scabbing (L4)		Perforation (L5)		Penetration (L1)		Penetration (L1)	
300°C												
	Scabbing (L4)		Perforation (L6)		Scabbing (L4)		Perforation (L5)		Penetration (L2)		Penetration (L1)	
500°C	Explosive spalling		Explosive spalling									
					Perforation (L5)		Perforation (L5)		Penetration (L3)		Penetration (L2)	
700°C	Explosive spalling		Explosive spalling									
					Perforation (L6)		Perforation (L6)		Penetration (L3)		Penetration (L3)	

strength of the samples.

The mix proportions for HP-HFRCC are presented in Table 2, with design strengths categorized into 100 MPa (Fc100 series) and 140 MPa (Fc140 series). Fiber contents were set at 0.15% for PP and 1% for SSF. Specimens were divided into three groups: unreinforced (N series), PP-reinforced (PP series), and hybrid-reinforced (PPSF series). Specimens were prepared using a twin-shaft mixer. Aggregates and binders were dry-mixed for 5 minutes, followed by the addition of water and superplasticizers for another 5 minutes. Fibers were incorporated during the final mixing stage. The fresh mixture achieved a slump flow of 600±50 mm before being cast into molds. The specimens were steam-cured at 60°C for 3 days and then further cured at 22±2°C and 60% relative humidity for 28 days.

The thermal degradation test was conducted using the electric furnace shown in Fig. 2, targeting six temperature levels: 25°C (room temperature), 100°C, 200°C, 300°C, 500°C, and 700°C. The specimens were heated at a rate of 1°C/min, and each target temperature was maintained for a specific duration. A maximum temperature of 700°C was set as the experimental limit, reflecting realistic disaster conditions; temperatures beyond this point were excluded due to rapid degradation and specimen failure, which made quantitative evaluation impractical. Compressive and tensile strengths were evaluated at each temperature level, along with impact resistance tests.

High-speed projectile impact tests were conducted using the apparatus shown in Fig. 3. The system used nitrogen gas to launch a steel spherical projectile (25 mm in diameter, 66.7 g in mass) at a velocity of approximately 210 m/s, delivering a kinetic energy of 1,470 J.

Specimens, measuring 200×200 mm, were tested with thicknesses of 40 mm, 60 mm, and 80 mm. After impact, the diameter of the crater and fracture depth were measured as shown in Fig. 4.

The fracture mode was classified into six levels (L1–L6). L1 indicates surface penetration, L2 rear surface cracking, L3 rear surface deformation, L4 rear surface spalling (scabbing), L5 complete perforation, and L6 complete projectile penetration. These six levels were derived by subdividing the three fundamental fracture modes—Penetration, Scabbing, and Perforation—into more detailed stages to enable a more nuanced qualitative evaluation. Specifically, Penetration was subdivided into L1 to L3, Scabbing corresponds to L4, and Perforation was subdivided into L5 and L6. These damage levels were used to qualitatively evaluate the residual impact resistance of the specimens.

3. RESULTS AND DISCUSSION

Tables 3, 4, and 5 illustrate the impact failure conditions of specimens subjected to high-temperature heating, followed by impact loading, based on thicknesses of 40, 60, and 80 mm. The results of evaluating impact resistance performance after high-temperature heating reveal significant differences in impact resistance depending on fiber reinforcement and mixing methods. Impact failure levels were categorized into penetration, scabbing, and perforation modes, and the effects of specimen thickness and heating temperature on impact resistance were analyzed.

For specimens with a thickness of 40 mm (Table 3), explosive spalling occurred in non-fiber-reinforced specimens (Fc100N and Fc140N) at temperatures above 500°C,

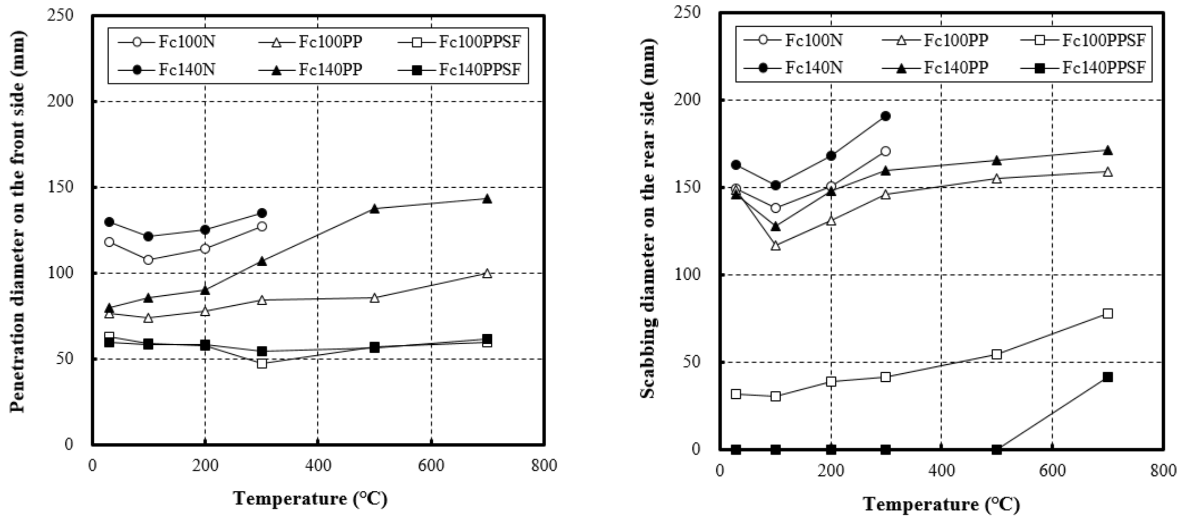

(a) Penetration diameter (b) Scabbing diameter

Fig.5 Crater diameter

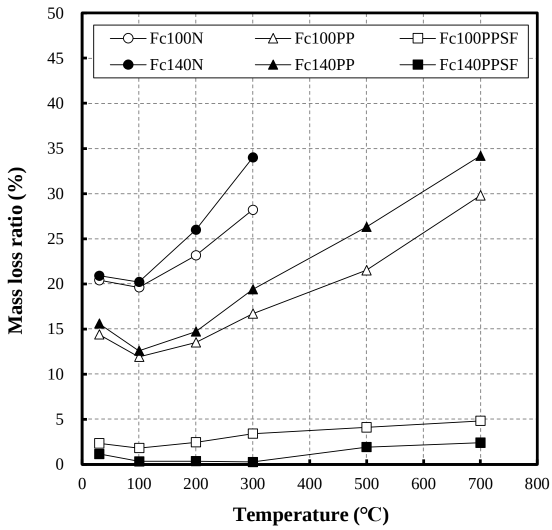

Fig.6 Mass loss ratio

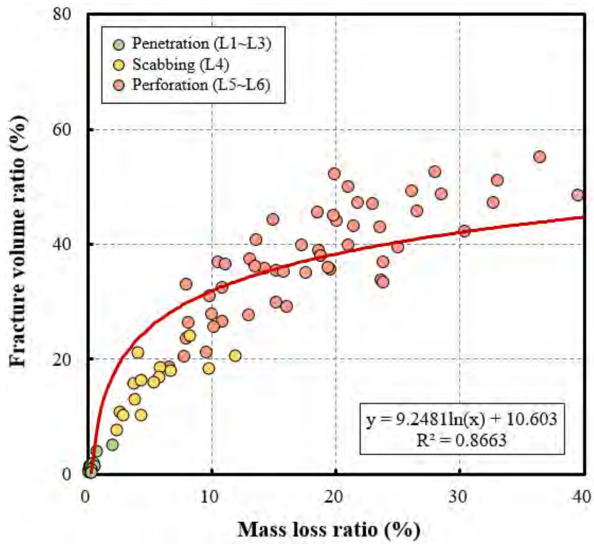

Fig.7 Mass loss-fracture volume ratio correlation

exhibiting L6-level penetration failure. Specimens with PP (Fc100PP and Fc140PP) prevented explosive spalling but showed the same L6 failure mode. On the other hand, specimens with hybrid reinforcement of PP and SSF (Fc100PPSF and Fc140PPSF) did not experience penetration failure up to 300°C. Notably, Fc140PPSF maintained high impact resistance without scabbing on the rear face even at 500°C, demonstrating the significant contribution of steel fiber reinforcement to improving impact resistance. However, at 700°C, perforation modes were observed in all specimens.

For specimens with a thickness of 60 mm (Table 4), the failure levels of non-reinforced specimens (Fc100N and Fc140N) were similar to those of 40 mm specimens, despite the increase in thickness. In PP-reinforced specimens, Fc100PP exhibited reduced failure levels to rear scabbing (L4) within the 200°C–300°C range. However, Fc140PP, despite its higher strength, showed L6 penetration failure and severe damage. Hybrid fiber-reinforced specimens (Fc100PPSF and Fc140PPSF) exhibited significantly reduced failure levels with increasing thickness. In particular, Fc140PPSF suppressed rear scabbing up to 700°C, showing only L2–L3 levels of damage across all temperature ranges.

For specimens with a thickness of 80 mm (Table 5), non-reinforced and PP-only reinforced specimens showed partial improvement in failure levels with increasing thickness. However, Fc140N and Fc140PP still exhibited L5–L6 penetration failure at temperatures above 100°C. In contrast, hybrid fiber-reinforced specimens (Fc100PPSF and Fc140PPSF) demonstrated excellent impact resistance, maintaining no rear scabbing from 25°C to 700°C. Specifically, Fc140PPSF sustained L1 levels of damage up to 300°C and benefited significantly from the synergistic effects of higher strength and increased thickness in enhancing impact resistance.

Fig. 5 illustrates the changes in the front penetration diameter and rear scabbing diameter of cement composites with increasing temperature. Specimens without fiber reinforcement (Fc100N, Fc140N) and those containing only PP (Fc100PP, Fc140PP) showed an increasing trend in both penetration and scabbing diameters as the temperature rose, with this increase being more pronounced at higher temperatures. In contrast, hybrid-reinforced specimens incorporating PP and SSF (Fc100PPSF, Fc140PPSF) maintained relatively smaller penetration and scabbing diameters, with minimal rear damage observed even at 700°C. These results indicate that hybrid reinforcement with PP and SSF significantly enhances resistance to high-temperature degradation and impact loads.

Fig. 6 presents the average mass loss rates of specimens subjected to high temperatures and impact loads. Specimens without fiber reinforcement (Fc100N, Fc140N) exhibited increased mass loss rates with rising temperatures. Notably, Fc140N, despite its higher design strength, showed greater mass loss due to its vulnerability to high-pressure steam. Specimens with PP reinforcement (Fc100PP, Fc140PP) demonstrated slightly reduced mass loss rates compared to non-reinforced specimens, but Fc140PP, with its denser matrix, remained more susceptible to mass loss than Fc100PP. In contrast, hybrid-reinforced specimens (Fc100PPSF, Fc140PPSF) showed remarkable suppression of mass loss rates, maintaining values below 5% across all temperatures. In particular, Fc140PPSF exhibited a low mass loss rate of approximately 3% even at 700°C. This performance is attributed to the synergistic effects of PP and SSF: the low melting point of PP induces a micro-crack network that reduces pore pressure, while SSF mitigates impact stress and bridges matrix gaps, effectively suppressing spalling and mass loss.

Fig. 7 illustrates the correlation between mass loss rates and fracture volume ratios for specimens subjected to high temperatures and impact loads. The study classified impact failure into three stages based on mass loss rates and fracture volume ratios. Surface penetration mode was observed when the mass loss rate was below 2% and the volume loss ratio was under 5%. Rear scabbing occurred within the ranges of a mass loss rate below 10% and a volume loss ratio below 20%. Penetration failure initiated at a mass loss rate of approximately 10% and a fracture volume ratio of about 20%, with maximum failure levels reaching approximately 40% and 55%, respectively. The impact failure of hybrid-reinforced specimens predominantly remained within the surface penetration stage.

In conclusion, hybrid reinforcement with PP and SSF significantly enhances the matrix's resistance to high-temperature degradation and impact loads, effectively suppressing mass loss and fracture volume while minimizing rear damage.

4. CONCLUSIONS

This study demonstrates the significant effectiveness of hybrid fiber-reinforced high-performance cementitious composites (HP-HFRCC) incorporating polypropylene fiber (PP) and smooth steel fiber (SSF) under high-temperature and high-velocity impact conditions. The following conclusions can be drawn:

(1) Hybrid-reinforced specimens (Fc100PPSF and Fc140PPSF) exhibited superior resistance to thermal degradation and dynamic loads compared to non-reinforced and PP-only reinforced specimens. The hybrid combination of PP and SSF effectively minimized penetration diameters, rear scabbing, and fracture levels across a wide range of temperatures (25°C–700°C).

(2) The inclusion of hybrid fibers significantly reduced mass loss rates. In particular, Fc140PPSF maintained a mass loss rate of approximately 3% at 700°C, demonstrating excellent thermal stability and structural integrity. This result is attributed to the synergistic effects of PP fibers and SSF in reducing pore pressure and mitigating impact stresses.

(3) Hybrid fibers provided a synergistic improvement in resistance to thermal and impact loads. The combination of the low melting point of PP fibers and the mechanical bridging effect of SSF minimized spalling and cracking, even under extreme conditions.

(4) The hybrid-reinforced composites maintained their protective capabilities even at reduced thicknesses. Damage predominantly remained in the surface penetration stage, indicating the material's potential for applications requiring thin, high-strength protective layers.

These findings highlight the applicability of HP-HFRCC in enhancing the resilience of smart city infrastructures against disaster scenarios. Further research into optimizing fiber content and examining long-term performance under multi-hazard conditions can provide more comprehensive data for practical implementation.

ACKNOWLEDGEMENT

This work was supported by the Korea Planning & Evaluation Institute of Industrial Technology(KEIT) grant funded by the Korea government(MSIT) (RS-2024-00417276).

REFERENCES

[1] Q. Hassan, A.Z. Sameen, O. Olapade, M. Alghoul, H.M. Salman, M. Jaszczur, Hydrogen fuel as an important element of the energy storage needs for future smart cities, Int. J. Hydrogen Energy. 48 (2023) 30247–30262.

[2] Y. Meduri, R. Singh, G. Manoharan, Key networks to create disaster resilient Smart Cities Mission: A case for remodeling India’s Smart Cities Mission to include disaster resilience, Resilient Cities Struct. 3 (2024) 52–62.

[3] M. Pagani, W. Korosec, N. Chokani, R.S. Abhari, User behaviour and electric vehicle charging infrastructure: An agent-based model assessment, Appl. Energy. 254 (2019) 113680.

[4] R. Gupta, C. Mejia, Y. Gianchandani, Y. Kajikawa, Analysis on formation of emerging business ecosystems from deals activities of global electric vehicles hub firms, Energy Policy. 145 (2020) 111532.

[5] K.G. Logan, J.D. Nelson, X. Lu, A. Hastings, UK and China: Will electric vehicle integration meet Paris agreement targets?, Transp. Res. Interdiscip. Perspect. 8 (2020).

[6] J. Liu, C. Wu, J. Li, Z. Liu, S. Xu, K. Liu, Y. Su, J. Fang, G. Chen, Projectile impact resistance of fibre-reinforced geopolymer-based ultra-high performance concrete (G-UHPC), Constr. Build. Mater. 290 (2021).

[7] K. Habel, M. Viviani, E. Denarié, E. Brühwiler, Development of the mechanical properties of an Ultra-High Performance Fiber Reinforced Concrete (UHPFRC), Cem. Concr. Res. 36 (2006) 1362–1370.

[8] L. Shen, X. Yao, G. Di Luzio, M. Jiang, Y. Han, Mix optimization of hybrid steel and polypropylene fiber-reinforced concrete for anti-thermal spalling, J. Build. Eng. 63 (2023) 105409.